JOURNAL OF Applied Polymer SCIENCE

Electrospun Polyaniline Nanofibers Web Electrodes for Supercapacitors

Sudeshna Chaudhari,[1] Yogesh Sharma,[2] Panikar Sathyaseelan Archana,[3] Rajan Jose,[4] Seeram Ramakrishna,[3] Subodh Mhaisalkar,[5] Madhavi Srinivasan[1,5]

[1]School of Materials Science and Engineering, Nanyang Technological University, Singapore 639798, Singapore
[2]Physics Section, Department of Paper Technology, Indian Institute of Technology, Saharanpur, Uttar Pradesh 247001, India
[3]Nanoscience and Nanotechnology Initiative, National University of Singapore, Singapore 174576, Singapore
[4]Faculty of Industrial Science and Technology (FIST), Universiti Malaysia Pahang, 26300 Kuantan, Malaysia
[5]Energy Research Institute @ NTU (ERI@N), Singapore 637553, Singapore
Correspondence to: M. Srinivasan (E-mail: madhavi@ntu.edu.sg)

ABSTRACT: Polyaniline nanofibers (PANI-NFs) web are fabricated by electrospinning and used as electrode materials for supercapacitors. Field-emission scanning electron microscope micrographs reveal nanofibers web were made up of high aspect ratio (>50) nanofibers of length ~30 μm and average diameter ~200 nm. Their electrochemical performance in aqueous (1*M* H_2SO_4 and Na_2SO_4) and organic (1*M* $LiClO_4$ in propylene carbonate) electrolytes is compared with PANI powder prepared by *in situ* chemical oxidative polymerization of aniline. The electrochemical properties of PANI-NFs web and PANI powder are studied using cyclic voltammetry, galvanostatic charge/discharge, and electrochemical impedance spectroscopy. PANI-NFs web show higher specific capacitance (~267 F g^{-1}) than chemically synthesized PANI powder (~208 F g^{-1}) in 1*M* H_2SO_4. Further, PANI-NFs web demonstrated very stable and superior performance than its counterpart due to interconnected fibrous morphology facilitating the faster Faradic reaction toward electrolyte and delivered specific capacitance ~230 F g^{-1} at 1000th cycle. Capacitance retention of PANI-NFs web (86%) is higher than that observed for PANI powder (48%) indicating the feasibility of electro spun PANI-NFs web as superior electrode materials for supercapacitors. © 2012 Wiley Periodicals, Inc. J. Appl. Polym. Sci. 129: 1660–1668, 2013

KEYWORDS: conducting polymers; electrospinning; batteries and fuel cells; coatings; fibers

Received 8 October 2012; accepted 20 November 2012; published online 18 December 2012
DOI: 10.1002/app.38859

INTRODUCTION

Global warming, depletion of conventional energy sources, and increasing energy needs of modern world have redirected attention not only to produce clean, sustainable energy (e.g., wind, solar) but also on diverse class of energy storage devices that can efficiently store energy from these intermittent renewable energy sources.[1] Supercapacitor exhibiting 20–200 times greater capacitance and energy density (80–100 F g^{-1}, 5 W h kg^{-1}) than conventional capacitors and delivering higher power density (10 kW kg^{-1}) than batteries, represent an unique class of technology with niche applications amongst other energy storage devices. Supercapacitors have the advantages of stable cycle life and faster energy release at high rate as compared with lithium ion batteries, but their applications are restricted by their limited energy density.[2–4] Metal oxides and organic conducting polymers have been considered as promising candidates to conventional carbon-based electrodes (electric double layer capacitor) in supercapacitors due to their ability to deliver higher capacitance as a consequence of redox reactions (known as "pseudo-capacitance").[5–7]

Among the conducting polymers, polyaniline (PANI) is considered as a promising electrode materials for supercapacitors because of its environmental stability, controllable electrical conductivity multiple intrinsic redox states, and excellent processability.[8] However, the electrochemical performance of bulk PANI is limited due to the low electroactive contact surface area with electrolyte. Hence, 1D nanostructures of PANI, with different morphologies (such as nanowire, nanotube, nanofibers, nanowebs, etc.) are recognized to be beneficial in enhancing its electrochemical characteristics (rate capability, capacitance) due to the high accessible surface area, shorten diffusion length, structural integrity, and conducting pathways. Nanofibers of pristine PANI or composite with single walled carbon nanotubes, multiwalled carbon nanotubes (MWCNT), and graphene[9–11]

have been fabricated by different methods such as template synthesis,[12–14] stepwise electrochemical deposition,[15] and dilute chemical polymerization.[16] Nevertheless, these synthesis methods involves post removal of templates by dissolution and results in low aspect ratio nanofibers.

Electrospinning is a simple, scalable facile route of making high aspect ratio nanofibers with controllable diameter using electrostatic force.[17–19] Electrospun nanofibers combine a number of physical properties such as guided electron transport, strain-induced electronic properties, high mechanical strength, high degree of flexibility, large specific surface area, high electron and thermal diffusivity, and tailorable pore distribution which are very attractive properties for supercapacitor electrodes.[19–21]

To the best of our knowledge, there are no reports on electrospun PANI-nanofibers (NFs) web as electrode materials for supercapacitor applications. Direct processing of PANI-NFs web by electrospinning is a main challenge, and herein, we have overcome this by fabricating high aspect ratio >50 PANI-NFs web by electrospinning a polymeric blend of PANI with polyethylene oxide (PEO). Their performance in aqueous electrolyte (1*M* H_2SO_4 and 1*M* Na_2SO_4) and organic (1*M* $LiClO_4$ in propylene carbonate (PC)) electrolytes is compared with PANI powder prepared by *in situ* chemical oxidative polymerization of aniline. A comparative electrochemical study was carried out using cyclic voltammetry (CV), galvanostatic charge–discharge cycling (GCD), and electrochemical impedance spectroscopy (EIS).

EXPERIMENTAL

Materials

Analytical grade chemicals were used throughout this study. Polyaniline emeraldine base (PANI, M_w = 65,000), PEO (M_w = 100,000), 10-camphorsulfonic acid (HCSA), chloroform (HPLC grade), ammonium persulfate ($(NH_4)_2S_2O_8$), hydrochloric acid (HCl), and aniline ($C_6H_5NH_2$) were purchased from Aldrich. These chemicals were used without further purification.

Synthesis

Preparation of PANI-NFs Web. The sol for electrospinning was prepared using PANI (M_w = 65,000), chloroform, PEO (M_w = 100,000), and camphorsulfonic acid. The polymeric solution was prepared by dissolving PANI (0.7 g) in chloroform (1.95 wt %) followed by the addition of camphorsulfonic acid (0.15 g) to the PANI solution. The resulting sol was contained in an air-tight bottle and stirred for 24 h to form homogeneous and transparent solution and then filtered. Thereafter, 0.7 g PEO was added and again stirred for 24 h before electrospinning. Figure 1 shows the schematic of electrospinning set-up used. The composite solution was placed in a 5-mL plastic syringe with a capillary tip ($D \sim$ 12 mm). Electrospun PANI-NFs web were collected by attaching this to aluminum current collector at an applied voltage ~20 kV. The distance between collector and needle was ~10 cm and the feed rate of the solution was 1 mL h^{-1}. After electrospinning, PANI-NFs web were stored in vacuum box to avoid air contact.

Preparation of PANI Powder. PANI powder was synthesized by a standard chemical polymerization method in which an aqueous monomer solution containing 1*M* HCl and 0.1*M* monomer was prepared and cooled in an ice bath up to 0–5°C under constant stirring. After 2 h, the aqueous solution of oxidant, 0.1*M* ammonium persulfate was slowly added to the monomer solution to carry out the polymerization process up to 20 h. Subsequently, the solution was filtered and washed with deionized water repeatedly to remove the impurities and finally washed with 1*M* HCl solution to obtain dark green precipitate. Further, the precipitate was dried under dynamic vacuum at 60°C for 24 h.

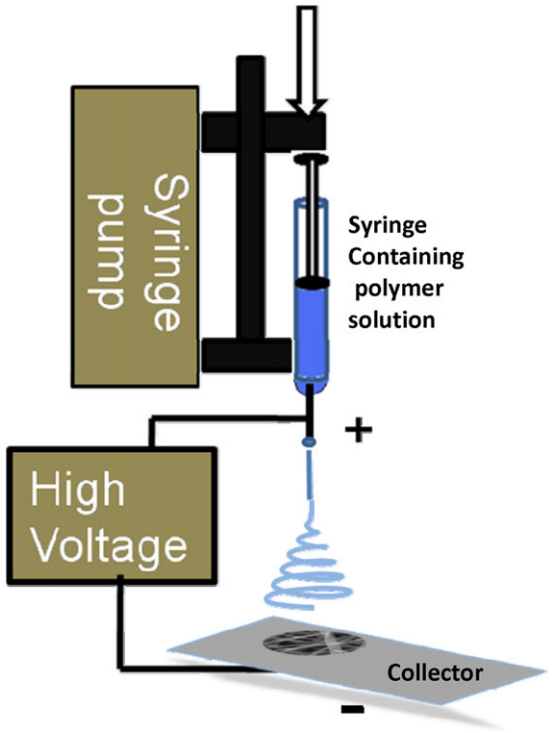

Figure 1. Schematic of electrospinning set-up. [Color figure can be viewed in the online issue, which is available at wileyonlinelibrary.com.]

Characterization of PANI-NFs Web and PANI Powder

Surface morphology of electrospun PANI-NFs web and chemically synthesized PANI powder was examined by field-emission scanning electron microscope (FE-SEM, JSM 6340) operating at 5 kV. The samples for FE-SEM were prepared by sputter coating with platinum for 60 s to minimize the charging effect. Transmission electron microscopy (TEM) images were captured (TEM, JEOL 2100F) by dispersing the sample in ethanol on a carbon-coated copper grid. Fourier transform infrared (FTIR) spectra were recorded with Perkin Elmer spectrometer (1600 Series II, USA) in the spectral range of 4000–400 cm^{-1}, using the KBr pellet method.

Electrode Fabrication and Electrochemical Characterization

The electrodes were prepared by mixing 75 wt % PANI-NFs web/powder as an active material (~3 mg), 15 wt % carbon black (super P from Timcal), and 10 wt % polyvinylidene fluoride, and few drops of *N*-methylpyrrolidinone as a solvent was added to form uniform slurry. The resulting uniform slurry was coated onto graphite substrate that served as current collector

Applied Polymer SCIENCE

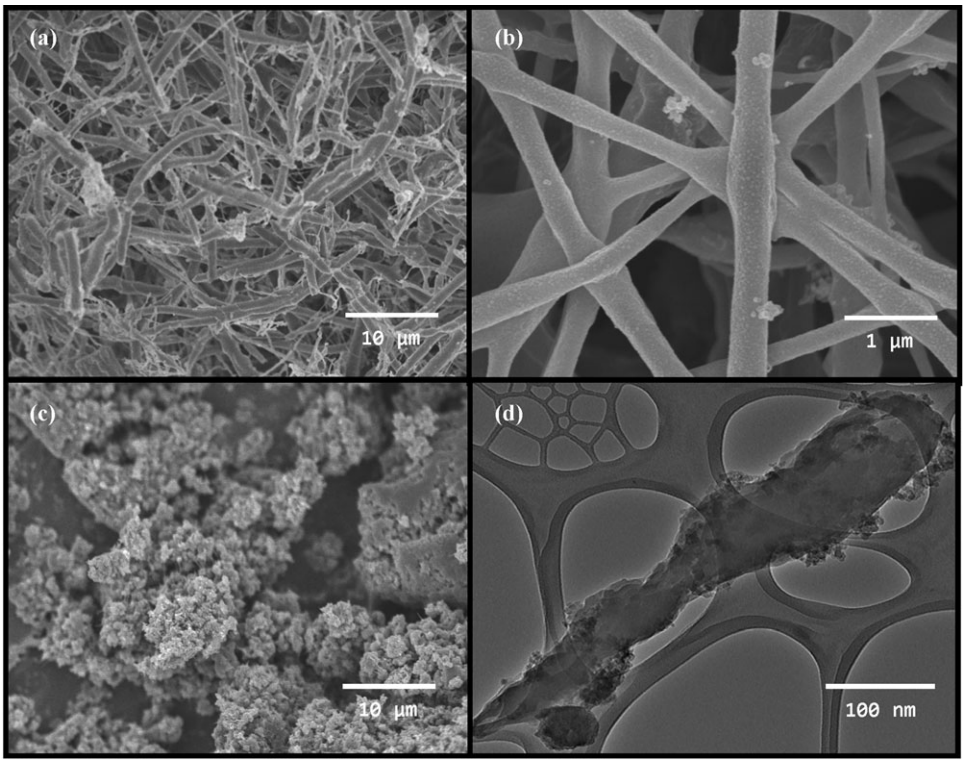

Figure 2. FESEM images of as-synthesized PANI-NFs web at (a) lower and (b) higher magnification and (c) as synthesized PANI powder and (d) TEM image of electrospun PANI-NFs web.

(1.5 cm^2). The coated PANI-NFs web/powder electrodes were dried at 80°C overnight in vacuum oven. The electrochemical performances of the electrodes were characterized by CV, GCD measurements, and EIS. The electrode performances were tested in aqueous (1*M* H_2SO_4 and 1*M* Na_2SO_4) and organic (1*M* $LiClO_4$ in PC). The CV experiments were carried out using a three-electrode geometry, in which platinum (50 cm^2) and the saturated calomel electrode were used as counter and reference electrodes, respectively. The cycling range was −0.3 to 0.6 V for aqueous electrolytes, whereas −0.6 to 1.2 V cycling range was used for organic electrolyte. We have optimized this particular region because the redox behavior for PANI electrode is observed only in this range. All the electrochemical measurements were carried out using a computer controlled potentiostat (Solartron, 1470E). The GCD properties were measured in two electrode geometry in the potential range of 0–1 V at the different current densities of 0.35, 1, and 1.67 A g^{-1}, respectively.

The EIS measurements were carried out at the open-circuit potential by using Solartron, SI 1255B Impedance/gain-phase analyzer at room temperature. The frequency was ranged from 0.1 Hz to 20 kHz with amplitude of superimposed AC signal of 10 mV. EIS curves of PANI-NFs web and powders under positive polarization show open circuit potential 0.060 and 0.014 V in aqueous 1*M* H_2SO_4, 0.005 and 0.016 V in 1*M* Na_2SO_4, and 0.0007 and 0.009 V in organic 1*M* $LiClO_4$ in PC electrolytes, respectively. The analysis of the impedance spectra was done by fitting the experimental results to equivalent circuits using Z-view software from Scribner Associates. The quality of fitting to equivalent circuit was judged first by the chi-square value (χ^2, i.e., the sum of the square of the differences between theoretical and experimental points) and second by limiting the relative error in the value of each element in the equivalent circuit to 5%.

RESULTS AND DISCUSSION

Morphology of PANI-NFs Web and Powders

Figure 2 shows the FE-SEM and TEM images of as-synthesized electrospun PANI-NFs web and powder, respectively. The FE-SEM images reveal the highly interconnected web of electrospun PANI-NFs as clearly shown in Figure 2(a,b), respectively. These nanofibers web have aspect ratio >7 and diameter lies in the distribution range of 100–400 nm, with an average of 200 nm. Moreover, the fibers form an interconnected web with the nanofibers on top of each other. The FE-SEM image of PANI powder prepared by chemical oxidative polymerization method, as shown in Figure 2(c), indicates the granular surface morphology of agglomerated particles (∼70–100 nm). The advantage of interconnected of PANI-NFs web allow easy access of electrolyte through the active polymer material as well as optimal for the fast ion diffusion and migration in the polymer by increasing more active reaction sites available for the Faradaic reaction, prerequisite for the supercapacitors.[22] The TEM image [Figure 2(d)] of as-synthesized single PANI-NFs web shows small particles of PANI attached on the surface of nanofibers, which might have been unprocessed during elongation and drying process. However, the particles to fiber ratio seem relatively low indicating that the PANI-NFs web is successfully prepared by using electrospinning process.

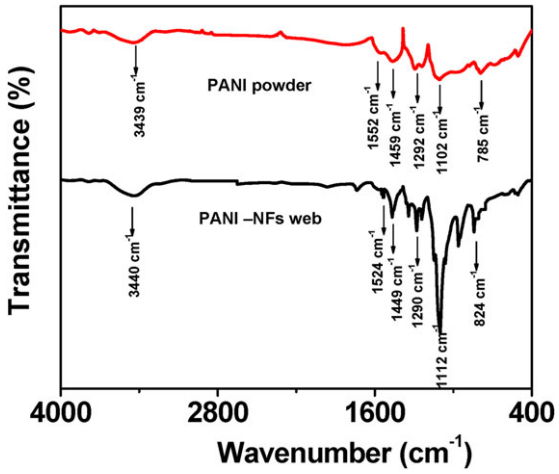

Figure 3. FTIR spectra of (a) PANI powder and (b) PANI-NFs web. [Color figure can be viewed in the online issue, which is available at wileyonlinelibrary.com.]

The FTIR spectra of PANI-NFs web and PANI powder are shown in Figure 3. The main characteristic bands of PANI are assigned as follows[23,24]: a broad band at 3439 cm^{-1} is due to the N—H stretching mode, the C=N and C=C stretching modes for the quinoid and benzoid rings occur at 1552 and 1459 cm^{-1}, respectively. The bands at 1292, 1102, and 785 cm^{-1} assigned to the C—N stretching of the secondary aromatic amine, C—H in plane bending and out of plane C—H bending vibration, respectively. This is a typical PANI spectrum, in accordance with those reported in the literature. The bands at 1524, 1449, 1290, and 1112 cm^{-1}, corresponding to the stretching modes of C=N, C=C, and C—N, are shifted to lower wave numbers, which may be attributed to the presence of PEO in the PANI matrix.

Electrochemical Performance of PANI-NFs Web and PANI Powder

To evaluate the electrochemical characteristics of PANI-NFs web as electrode materials for supercapacitors, the CV and GCD measurements were used and their results are compared with chemically synthesized PANI powder. The effect of different electrolytes such as aqueous (1*M* H_2SO_4 and 1*M* Na_2SO_4) and organic electrolyte (1*M* $LiClO_4$ in PC) on the electrochemical performance of PANI-NFs web and PANI powder is investigated. The corresponding CV curves, recorded at the scan rate of 5 mV s^{-1} in three electrode configurations, are shown in Figure 4. Considerable differences in the electrochemical behavior for PANI-NFs web as well as for PANI powder were observed in aqueous (acidic and neutral) electrolytes. As clearly shown in Figure 4(a), the pair of two redox peaks is observed in 1*M* H_2SO_4, which are attributed to the redox transition of PANI between leucoemeraldine form and polaronic emeraldine form as well as the emeraldine-pernigraniline transformation.[25]

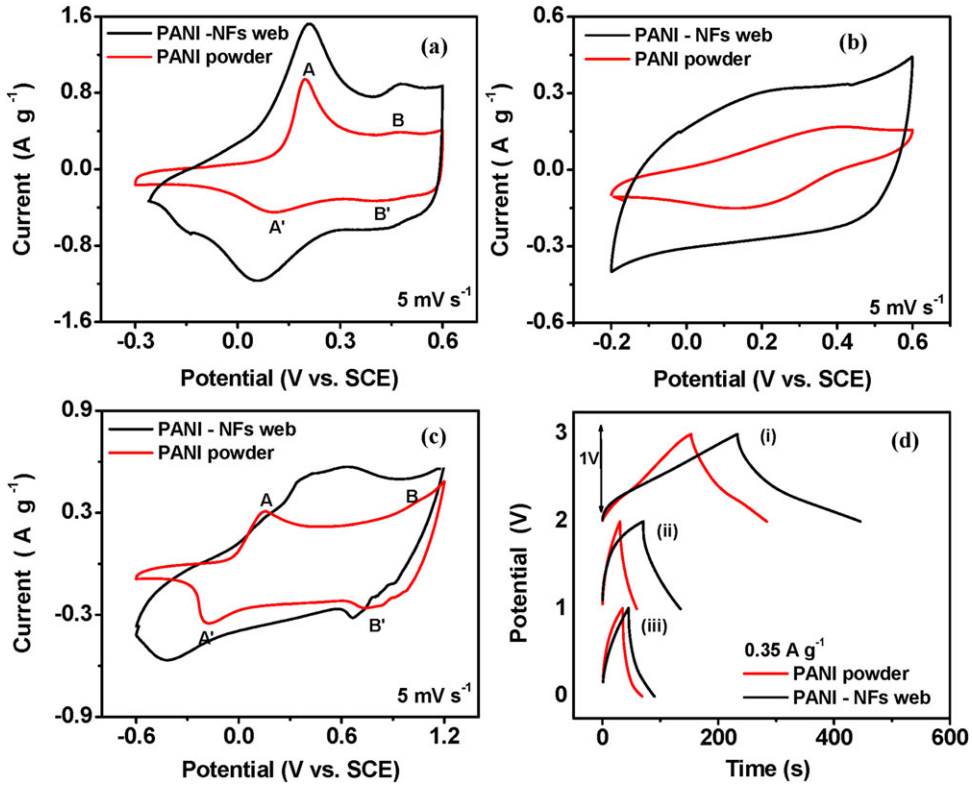

Figure 4. Cyclic voltammogram of the electrospun PANI-NFs web and PANI powder electrodes at the scan rate of 5 mV s^{-1} in (a) 1*M* H_2SO_4, (b) 1*M* Na_2SO_4, (c) 1*M* $LiClO_4$ in PC electrolyte, and (d) comparison of galvanostatic charge–discharge curves of electropsun PANI-NFs web and PANI powder electrodes at 0.35 A g^{-1} in (i) 1*M* H_2SO_4, (ii) 1*M* Na_2SO_4, and (iii) 1*M* $LiClO_4$ in PC, respectively. [Color figure can be viewed in the online issue, which is available at wileyonlinelibrary.com.]

Table I. The Specific Capacitance of PANI-NFs Web and PANI Powder in Various Electrolytes

	Electrolyte					
	1*M* H_2SO_4		1*M* Na_2SO_4		1*M* $LiClO_4$ in PC	
Current density (A g^{-1})	PANI-NF webs (F g^{-1})	PANI powder (F g^{-1})	PANI-NF webs (F g^{-1})	PANI powder (F g^{-1})	PANI-NF webs (F g^{-1})	PANI powder (F g^{-1})
0.35	267	208	52	48	112	98

The current density of the redox peaks is observed to be higher in PANI-NFs web as compared with the PANI powder, indicating the huge pseudocapacitance originating mainly due to the fast faradic reaction at the electrode surface.

The CV curves of PANI-NFs web as well as PANI powder in the 1*M* Na_2SO_4 electrolyte are shown in Figure 4(b) and reveal a little deviation from rectangular shape, whereas an improvement in the current density is noticed for PANI-NFs web. This further confirms the importance of interconnected nanofibrous morphology over agglomerated powder as electrode materials for supercapacitor applications.

To understand the electrochemical characteristics of the PANI-NFs web and PANI powder, we have also recorded the CV of these electrodes in organic electrolyte 1*M* $LiClO_4$ in PC and illustrated in [Figure 4(c)]. In case of PANI powder, two redox peaks (A, A′ and B, B′) are observed, whereas for PANI-NFs web the asymmetric shape of CV is observed. When compared with the PANI powder, the current density is higher in PANI-NFs web and the peaks are also shifted to lower potentials which indicate facile intercalation and deintercalation of Li^+ ion in PANI-NFs web.

The corresponding CV curves for PANI-NFs web and powder in different electrolytes can be correlated with the conductivity of a particular electrolytes system, which is the sum of the conductivities of individual ions present in it. The important factors influencing the conductivity include the charge and size of the individual ions. Because small ions move through electrolyte more rapidly than larger ions, their conductivity in electrolytes is expected to be higher. Comparing the conductivities of different electrolytes, i.e., H_2SO_4, Na_2SO_4, and $LiClO_4$ in which SO_4^{2-} ions are the same for the aqueous systems, has enabled the conductivities of individual ions (H^+, Na^+, and Li^+) to be determined. Smaller ion hydration number and effective radius of H^+ ions makes them more electroactive than Na^+ (~4.7) and Li^+ (~5.3) ions, which produces larger electrochemical current response, whereas smaller ion hydration number and effective radius of ClO_4^- than SO_4^{2-} ions make them less electroactive.[26,27] Thus, the conductivity of electrolytes can be arranged in decreasing order, i.e., 1*M* H_2SO_4 > 1*M* $LiClO_4$ in PC > 1*M* Na_2SO_4. Because of the higher conductivity of 1*M* H_2SO_4 electrolyte system compared with other electrolytes, the current density of PANI-NFs web as well as powder electrodes is observed to be higher in acidic electrolytes.

The current density of PANI-NFs web observed is higher as compared with PANI powder in all three electrolyte systems. This can be attributed to the interconnected nanostructured PANI-NFs web that would facilitate facile electron conduction pathway originating from ("pseudo-capacitance") involving counter ion insertion/extraction from the polymer.

Figure 4(d) represents the typical GCD curves of PANI-NFs web and PANI powder in aforementioned electrolytes at constant current density of 0.35 A g^{-1} between 0 and 1 V in symmetric configuration (two electrode geometry). As clearly seen for PANI powder, potential varies nearly linear with time, whereas PANI-NFs web electrode show small deviation in the slope of the line with time. This exhibits the relationship with the peak B and B′ (redox conversion of emeraldine/pernigraniline) in the CV curves of 1*M* H_2SO_4 (Ref. 9) and is more prominent in the nanofibers leading to the high capacitance observed.

The specific capacitance "C_s" can be calculated from charge/discharge curves according to the following equation[28]

$$C_s = \frac{2I}{m\frac{dv}{dt}} \quad (1)$$

where C_s is the specific capacitance, I is the applied current, m is the total mass of the active material, and dv/dt is the slope of the discharge curve. The calculated initial specific capacitance values at constant current density of 0.35 A g^{-1} for different electrolytes are given in Table I. The difference of specific capacitance in three electrolytes is ascribed to the different properties of electrolytes and varying redox mechanisms. The calculated specific capacitance of PANI-NFs web at the current density of 0.35 A g^{-1} is 267 F g^{-1} which is higher than that of PANI powder (208 F g^{-1}). Based on the supercapacitive behavior of PANI electrodes in different electrolytes, a high conductivity of PANI in 1*M* H_2SO_4 than that in 1*M* Na_2SO_4 and 1*M* $LiClO_4$ in PC leads to a more sufficient use of electrode materials, and therefore, the specific capacitance is observed to be higher. The GCD results are complimentary to the CV results.

Electrochemical Impedance Spectroscopy. EIS has been used to compliment the results obtained from the CV and GCD studies. The Nyquist plots of the PANI-NF webs and PANI powder electrodes in aforementioned aqueous and organic electrolytes are measured and illustrated in Figure 5, which clearly indicates a small arc in high frequency region and a sloppy region in the middle to low frequency region. The charge transfer kinetics dictates at intermediate and high frequency ranges (20 kHz to 1 kHz), whereas ionic diffusion (mass transfer) rules in the low frequency range (1 kHz to 0.1 Hz).[29–34]

To elucidate the individual processes and therefore associated impedance parameters, an equivalent circuit comprising series

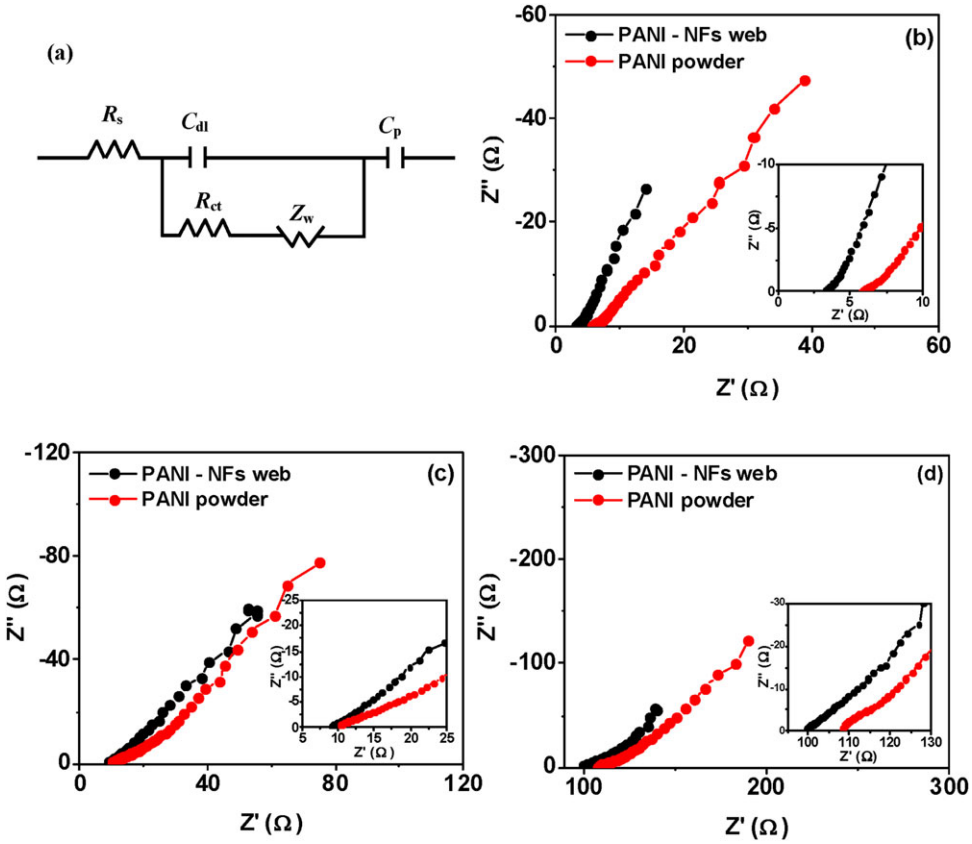

Figure 5. Equivalent circuit (a) and Nyquist impedance plots of the electrospun PANI-NFs web and PANI powder electrodes in (b) 1*M* H_2SO_4, (c) 1*M* Na_2SO_4, (d) 1*M* $LiClO_4$ in PC. Inset shows the high frequency region. [Color figure can be viewed in the online issue, which is available at wileyonlinelibrary.com.]

and parallel combinations of equivalent series resistance (R_s), electrical double layer capacitance (C_{dl}), charge transfer impedance (R_{ct}), frequency dependent Warburg impedance (Z_w), and pseudocapacitance (C_p) has been configured.[29,30] The data has been fitted to the equivalent circuit shown in Figure 5(a) and selected parameters are displayed in Table II. EIS gives the important information about the equivalent series resistance (R_s) (combination of electrolyte resistance, inter-particle resistance of electrode, and contact resistance, etc.).[29,30,32] The intersection of the plots at the *x*-axis represents the R_s, which determines the charge/discharge rate of the electrode.[33] The power density of any supercapacitor is inversely proportional to the series resistance.[33] From Figure 5(b–d) and Table II, the value of R_s is found to be minimum (~3.3 Ω) in the case of PANI-NF web with 1*M* H_2SO_4 electrolyte and increases slightly in 1*M* Na_2SO_4 and quite high for 1*M* $LiClO_4$ in PC. The lower value in former is ascribed to the high accessible surface area and good compatibility with the electrolytes used which makes PANI-NF web attractive electrode materials for supercapacitor. Higher values in later may hinder the facile ionic transport in these electrolytes[33] and, therefore, poor electrochemical properties are envisaged. Moreover, the inter-particle resistance seems higher in

Table II. Impedance Parameter Values Extracted from the Fit to the Equivalent Circuit for the Impedance Spectra Recorded in Various Electrolytes Solution

	Electrolyte					
	1*M* H_2SO_4		1*M* Na_2SO_4		1*M* $LiClO_4$ in PC	
Circuit parameters	PANI-NFs web	PANI powder	PANI-NFs web	PANI powder	PANI-NFs web	PANI powder
R_s (Ω)	3.3	5.9	9.0	10.5	99.0	110.1
C_{dl} (mF)	0.34	0.30	0.19	0.12	0.24	0.21
R_{ct} (Ω)	0.45	0.40	0.91	0.25	1.77	2.09
C_p (F)	0.62	0.58	0.23	0.21	0.56	0.51
Z_w (Ω $s^{-0.5}$)	0.65	0.64	0.78	0.72	0.97	0.96

Applied Polymer SCIENCE

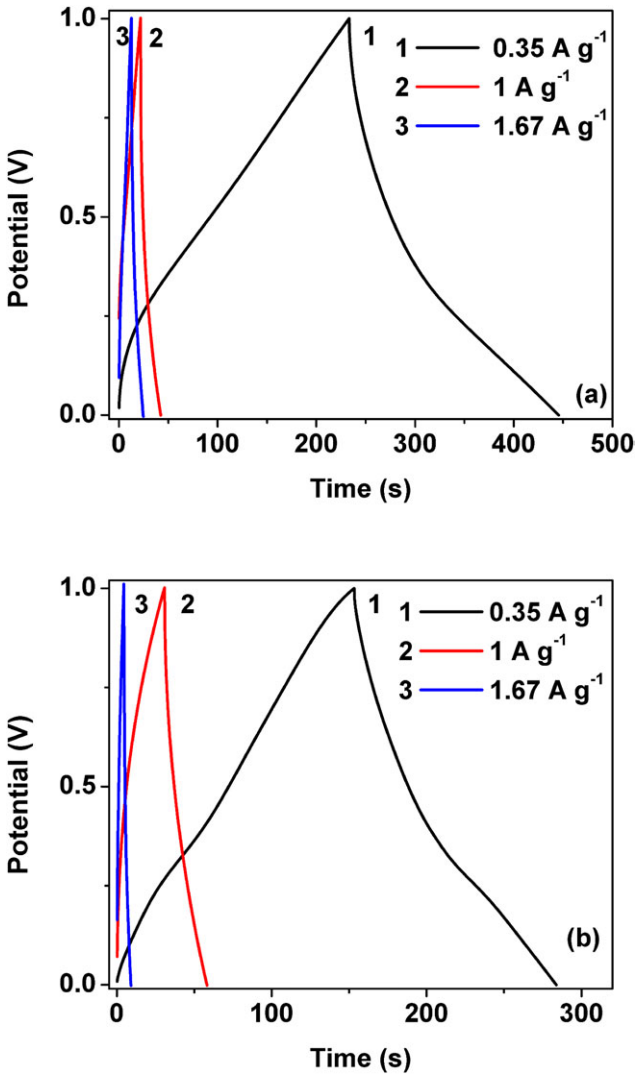

Figure 6. Galvanostatic charge–discharge curves recorded at different current densities 0.35, 1, and 1.67 A g^{-1} for (a) PANI-NFs web and (b) PANI powder in 1*M* H_2SO_4, respectively. [Color figure can be viewed in the online issue, which is available at wileyonlinelibrary.com.]

PANI powder as compared with the PANI-NF webs which may be due to the formation of agglomerated particles during synthesis.

For supercapacitors, the majority of the capacitance is available in low frequency region, so attention has also been paid to impedance data in middle to lower frequency region. In high frequency region, double layer capacitance is seems to be very small that reflects the poor penetration of electrolyte ions into the bulk or interior depth of the electrodes under high frequency.[32,33] It should be noted that the value of specific capacitance (assuming the weight of electrode ~3 mg) derived by EIS technique is different than the observed value by CV [Figure 4(a–c)] and GCD [Figure 4(d)] techniques. This difference may be attributed to the usage of different testing system and different experimental conditions. The capacitance values estimated by EIS for PANI-NF webs in all the electrolytes are found to be higher than the synthesized PANI powder. This further proves the significance of PANI-NF webs as electrode material for supercapacitor.

Further, the sloppy region at ~45° toward low frequency represents the Warburg impedance and is a result of frequency dependence ion diffusion/transport in the electrolyte.[29–31,33] Almost un-noticeable Warburg region for PANI-NF webs in 1*M* H_2SO_4 indicates the short ion diffusion path which facilitates the efficient access of electrolyte ions to the surface of PANI-NF webs.[33] Whereas the large regions of Warburg curve in other two electrolytes: 1*M* Na_2SO_4 and 1*M* $LiClO_4$ in PC shows a large variation in the ion diffusion path lengths and increased obstruction of ion movement. This results the poor supercapacitor behavior of PANI-based electrodes in these two electrolytes. Thus, in view of minimum R_s and small Warburg regions showed in EIS studies, PANI-NF webs are found to be superior over their counterpart PANI-powder.

Cycling Stability. The rate capability study is also conducted in the galvanostatic mode for PANI-NFs web and PANI powder in 1*M* H_2SO_4 electrolyte and given in Figure 6(a,b), respectively. In 1*M* H_2SO_4 electrolyte, GCD curves for PANI-NFs web slightly deviate from the linear characteristics, whereas linear for PANI powder at all current densities. However, PANI-NFs web as well as PANI powder electrodes are nearly symmetric at all current densities demonstrating that the electrodes display ideal capacitive properties in the potential range investigated.

The cycle stability of the PANI-NFs web and PANI powder electrodes are evaluated at the current density of 0.35 A g^{-1} using GCD measurements over 1000 cycles. The specific capacitance based on electroactive materials as a function of cycle number is shown in Figure 7. PANI-NFs web are found to exhibit excellent stability over the entire cycles. After the 1st cycle, the specific capacitance decreases up to 100th cycle and thereafter reaches to the stable capacitance value of 230 F g^{-1}. It can be seen in the initial cycles, PANI system experiencing capacitance fade (up to 100 cycles) and this is due to the equilibrium of both

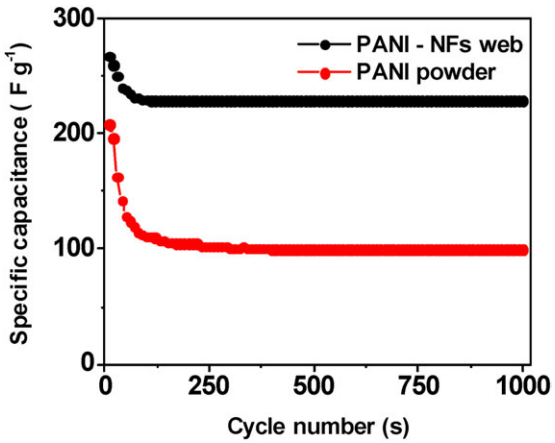

Figure 7. Specific capacitance of the electrospun PANI-NFs web and PANI powder electrodes in 1*M* H_2SO_4 at a current density of 0.35 A g^{-1} as a function of cycle number, respectively. [Color figure can be viewed in the online issue, which is available at wileyonlinelibrary.com.]

electrode potentials. Once the system is stabilized (beyond 100), no such fade is observed until 1000 cycles. For PANI powder, the specific capacitance decreases up to 20% is observed after 200 cycles (100 F g^{-1}) but after that reaches to the steady state. However, both electrodes are exhibiting the good cycleability after the stabilization of the electrode. It is seen that the capacitance retentions of PANI-NFs web and PANI powder over 1000 cycles are 86% and 48%, respectively. In PANI-NFs web, not only the high value of capacitance but also superior electrochemical cycleability is observed over 1000 cycles. This infers the importance of nanofibers web over agglomerated particles in terms of electrode morphology.

The observed cycleability and stability are consistent with the previous reports. For instance, Yan et al.[11] reported the synthesis of PANI by *in situ* polymerization process and obtained 115 F g^{-1} at 1 mV s^{-1} in 6*M* KOH; however, there is no cycleability was reported for pure PANI. Recently, Wu et al.[35] examined the graphene/PANI-NF system in 1*M* H_2SO_4 and revealed that both pure PANI and its composite experienced the severe fading. At the end of 800th cycle, 133 and 155 F g^{-1} is obtained for pure PANI and composite, respectively. Electrochemical polymerization of PANI on carbon substrate is reported by Chen et al.[36] and it delivered the capacitance of 180 F g^{-1} in H_2SO_4 with capacitance fade during the cycling. Kong et al.[37] adopted the chemical oxidative polymerization technique to synthesize the PANI along with multiwalled carbon nanotube (MWCNT) with different proportions in 1*M* $NaNO_3$ electrolyte. The 0.8 wt % MWCNT containing PANI electrode exhibited maximum specific capacitance of 224 F g^{-1}, whereas pure PANI showed only 178 F g^{-1} and there is no cycling data is available. It is observed that PANI-NFs web based supercapacitor exhibited good cycleability and rendered excellent retention than previous reports. These results confirmed that fabrication of electrodes using electrospun PANI-NFs web is the promising way to achieve high performance supercapacitors. To alleviate the fade in the initial cycles and improve the capacitance performance, the further research is underway using the electrospun PANI-NFs web.

CONCLUSIONS

The importance of interconnected PANI-NFs web, prepared by electrospinning over chemically synthesized agglomerated PANI particles, as electrode materials for supercapacitors in different electrolytes (made up of different cations and anions) is well-demonstrated. The specific capacitance of PANI-NFs web in 1*M* H_2SO_4 is 267 F g^{-1} at current density of 0.35 A g^{-1}, much higher as compared with PANI powder (208 F g^{-1}). Further, PANI-NFs web demonstrated very stable and superior performance than its counterpart and delivered the specific capacitance of 230 F g^{-1} at 1000th cycle. Over 86% of the original capacitance of the PANI-NFs web is retained after 1000 cycles, indicating a good cycle performance. The capacitance retention of the PANI powder is observed to be 48% after 1000 cycles, indicating that PANI-NFs web have better cycle stability. Smaller individual impedance parameters in case of PANI-NFs web are also observed, indicating the availability of electroactive sites needed for charge transfer reaction and counterion diffusion. Therefore, it is demonstrated that PANI-NFs web can be considered as a potential candidate for high-performance supercapacitors.

ACKNOWLEDGMENTS

The authors thank the grant from National Research Foundation, Singapore (NRF-CRP4-2008-03) and grant-in-aid RDU 100337.

REFERENCES

1. Subramanian, V.; Zhu, H.; Vajtai, R.; Ajayan, P. M.; Wei, B. *J. Phys. Chem. B* **2005**, *109*, 20207.
2. Conway, B. E. Electrochemical Supercapacitors; Kluwer Academic/Plenum Publishers: New York, **1999**.
3. Sarangpani, S.; Tilak, B. V.; Chen, B. V. *J. Electrochem. Soc.* **1996**, *143*, 3791.
4. Ju, Y. W.; Choi, G. R.; Jung, H. R.; Lee, W. J. *Electrochim. Acta* **2008**, *53*, 5796.
5. Jurewicz, K.; Delpeux, S.; Bertagna, V.; Beguin, F.; Frackowiak, E. *Chem. Phys. Lett.* **2001**, *347*, 36.
6. Frackowiak, E.; Beguin, F. *Carbon* **2001**, *39*, 937.
7. Zheng, J. P.; Cygan, P. J.; Jow, T. R. *J. Electrochem. Soc.* **1995**, *142*, 2699.
8. Kang, E. T.; Neoh, K. G.; Tan, K. L. *Prog. Polym. Sci.* **1998**, *23*, 277.
9. Liu, J.; Zhou, M.; Fan, L. Z.; Li, P.; Qu, X. *Electrochem. Acta* **2010**, *55*, 5819.
10. Deng, M.; Yang, B.; Hu, Y. *J. Mater. Sci.* **2005**, *40*, 5021.
11. Yan, J.; Wei, T.; Fan, Z.; Qian, W.; Zhang, M.; Shen, X.; Wei, F. *J. Power Sources* **2010**, *195*, 3041.
12. Cao, Y.; Mallouk, T. E. *Chem. Mater.* **2008**, *20*, 5260.
13. Martin, C. R. *Science* **1994**, *266*, 1961.
14. Parthasarathy, R. V.; Martin, C. R. *Chem. Mater.* **1994**, *6*, 1627.
15. Liang, L.; Liu, J.; Windisch, C. F.; Exarhos, G. J.; Lin, Y. H. *Angew. Chem. Int. Ed. Engl.* **2002**, *41*, 3665.
16. Chiou, N. R.; Lui, C. M.; Guan, J. J.; Lee, L. J.; Epstein, A. *J. Nat. Nanotechnol.* **2007**, *2*, 354.
17. Deitzel, J. M.; Kleinmeyer, J.; Harris, D.; Beck, N. C. T. *Polymer* **2001**, *42*, 261.
18. Fong, H.; Reneker, D. H.; Chun, I. *Polymer* **1999**, *40*, 4585.
19. Ramakrishna, S.; Jose, R.; Archana, P. S.; Nair, A. S.; Balamurugan, R.; Venugopal, J.; Teo, W. E. *J. Mater. Sci.* **2010**, *45*, 6283.
20. MacDiarmid, A. G. *Angew. Chem. Int. Ed. Engl.* **2001**, *40*, 2581.
21. Hoeben, F. J. M.; Jonkhejim, P.; Meijer, E. W.; Schenning, A. P. H. *J. Chem. Rev.* **2005**, *105*, 1491.
22. Zhang, H.; Cao, G. P.; Wang, W. K.; Yuan, K.; Xu, B.; Zhang, W. F.; Cheng, J.; Yang, Y. S. *Electrochim. Acta* **2009**, *54*, 1153.
23. Wu, J. H.; Tang, Q. W.; Li, Q. H.; Lin, J. M. *Polymer* **2008**, *49*, 5262.

24. Zengin, H.; Zhou, W. S.; Jin, J.; Czerw, R.; Smith, D. W.; Echegoyen, L.; Caroll, D. L.; Foulger, S. H.; Ballato, J. *Adv. Mater.* **2002**, *14*, 1480.

25. Wang, Y. G.; Li, H. Q.; Xia, Y. Y. *Adv. Mater.* **2006**, *18*, 2619.

26. Kielland, J. *J. Am. Chem. Soc.* **1937**, *59*, 1675.

27. Reddy, R. N.; Reddy, R. G. *J. Power Sources* **2006**, *156*, 700.

28. Reddy, A. L. M.; Ramaprabhu, S. *J. Phys. Chem. C* **2007**, *111*, 7727.

29. Ghaemi, M.; Ataherian, F.; Zolfaghari, A.; Jafari, A. *Electrochim. Acta* **2008**, *53*, 4607.

30. Sen, P.; De, A. *Electrochim. Acta* **2010**, *55*, 4677.

31. Wang, L.; Li, X.; Wang, X.; Yang, X.; Lu, L. *Curr. Appl. Phys.* **2010**, *10*, 1422.

32. Chen, Y. L.; Hu, Z. A.; Chang, Y. Q.; Wang, H. W.; Zhang, Z. Y.; Yang, Y. Y.; Wu, H. Y. *J. Phys. Chem. C* **2011**, *115*, 2563.

33. Yan, X.; Chen, J.; Yang, J.; Xue, Q.; Miele, P. *ACS Appl. Mater. Interfaces* **2010**, *2*, 2521.

34. Zang, J.; Bao, S. J.; Li, C. M.; Bian, H. J.; Cui, X. Q.; Bao, Q. L.; Sun, C. Q.; Guo, J.; Lian, K. R. *J. Phys. Chem. C* **2008**, *112*, 14843.

35. Wu, W.; Xu, Y.; Yao, Z.; Liu, A.; Shi, G. *ACS Nano* **2010**, *4*, 1963.

36. Chen, W. C.; Wen, T. C.; Teng, H. *Electrochem. Acta* **2003**, *48*, 641.

37. Kong, L. B.; Zhang, J.; An, J. J.; Lu, Y. C.; Kang, L. *J. Mater. Sci.* **2008**, *43*, 3664.